Isotope shifts and hyperfine structure of optical transitions in $^{147-150,152,154}$Sm II by fast-ion-beam–laser spectroscopy

P. Villemoes, M. Wang,* A. Arnesen, C. Weiler, and A. Wännström†
Department of Physics, Uppsala University, Box 530, S-751 21 Uppsala, Sweden
(Received 2 May 1994; revised manuscript received 28 November 1994)

In this paper isotope shifts (IS's) and hyperfine structure hfs in 16 transitions of singly ionized samarium are presented. The IS's, which, to our knowledge, have not been determined previously, and the hfs are measured by collinear fast-ion-beam–laser spectroscopy. The ions are excited from metastable levels in the $4f^6(^7F)5d$ configuration to levels in the $4f^5\,5d6s$? and $4f^6(^7F)6p$? configurations with laser light in the red and orange part of the visible spectrum. The IS's between the isotopes $^{147-150,152,154}$Sm II are measured for two transitions while the IS's between the even isotopes ^{148,150,152,154}Sm II are measured for the other 14 transitions. Three of the 14 transitions are not tabulated in the literature. Tentative compositions of the upper levels are evaluated from the IS's by using the sharing rule. The IS's measurements are also used in an absolute calibration of the acceleration voltage within an accuracy of 0.1%. The hfs of 10 levels are recorded. Corresponding magnetic-dipole and electric-quadrupole coupling constants, A and B factors, are evaluated. The A and B factors have not been determined before for three of the levels, and for the other levels they are determined with improved accuracy.

PACS number(s): 32.30.Jc, 32.10.Fn

I. INTRODUCTION

The inclusion of the kinetic energy of the nucleus in the calculation of atomic energy levels leads to isotope shifts (IS), i.e., somewhat different energy levels for different isotopes. This effect gives shifts only for lighter elements and is of the same order of magnitude as the hyperfine structure (hfs). If also the finite size of the nucleus as well as its shape are considered, this will lead to IS's which are substantial only in heavy elements. The two types of IS's are normally called mass shift (MS) and field shift (FS). Furthermore, the MS is conventionally divided in two parts, the normal mass shift (NMS), which is the reduced mass contribution, and the specific mass shift (SMS), originating from a change in the correlation between the electrons. The study of the FS has given valuable information about the structure of heavier nuclei, e.g., changes of the nuclear charge distribution between isotopes [1]. However, measurements of IS may also give information about electron structure [2,3], in particular configuration interaction (CI), through the sharing rule [2]. This procedure requires an evaluation of the FS and the SMS for the mixed configuration as well as for the pure configurations in which it is expanded. In this work, this method is used to determine tentative CI compositions of 13 levels in Sm II, which, in the literature [4], are designated as belonging to pure configurations.

There are 376 known levels of singly ionized samarium [4]. The lower even levels have been assigned to the configurations $4f^6(^7F)6s$ and $4f^6(^7F)5d$, but the composition of the odd levels is less known. The assigned levels in [4] belong to either of the $4f^6(^7F)6p$ and $4f^5 5d6s$ configurations. Pushpa *et al.* [5] determined the IS of 182 transitions and from the data they could confirm and reassign levels to the $4f^6(^7F)6p$ and to the $4f^5\,5d6s$ configuration. Configuration interaction with the $4f^5\,5d^2$ configuration was also discussed. In our work, the FS and SMS contributions to the IS are separated, and tentative assignments of the odd levels are derived using the sharing rule [2] on the FS and SMS. This investigation confirms the assignment in [5] for all levels but one, and also indicates substantial mixing with another configuration, possibly the $4f^5\,5d^2$.

IS's of many transitions from levels in the $4f^6(^7F)6s$, and some from the $4f^6(^7F)5d$ configurations, to levels in the $4f^5\,5d6s$? and $4f^6(^7F)6p$? configurations in Sm II have been determined previously by Fabry-Pérot interferometry on hollow cathode light sources [5–7]. The accuracy of about 0.5–3 mK (15–90 MHz) of such measurements is limited by the broad instrumental line profiles and the spectra are complex, since neutrals and ions of several isotopes are present in the light source. Fast-ion-beam–laser spectroscopy can provide isotopically pure spectra if an analyzing magnet is employed and, since the Doppler broadening of the spectral lines is reduced due to kinematic compression [8,9], an accuracy of 5–10 MHz can be obtained for IS measurements. In order to excite different isotopes within the same laser scan, different isotopes are switched into the beam line by changing the current through the analyzing magnet [10]. The resonances of the various accelerated isotopes are separated in frequency by the IS and the differential Doppler shift. The latter correction comes from the fact that different isotopes have different velocities due to the

*Permanent address: Shanghai Institute of Optics and Fine Mechanics, Academia Sinica, P.O. Box 800211, Shanghai 201800, People's Republic of China.
†Corresponding author's FAX: +46 18 18 35 24.

isotopes' different masses. In order to extract the IS, the differential Doppler shift has to be determined. This is usually done by a calibration of the acceleration voltage (e.g., [11–13]). Another method is to record spectra with the laser and ion beams parallel as well as antiparallel to each other [10,14]. In this scheme, the differences in first-order Doppler shift between accelerated ions with different masses cancel if the frequency differences between isotopes in the two geometries are added.

In this work both methods are used to determine the isotope shifts of sixteen transitions from levels in the $4f^6(^7F)5d$ configuration to levels in the $4f^5\,5d6s$? and $4f^6(^7F)6p$? configurations. Two transitions are recorded in both the parallel and antiparallel geometry. We have used these measurements in a new approach to calibrating the ion velocity, equivalent to the acceleration voltage. The ion velocity can be accurately determined if the frequency differences between isotopes in the two geometries are subtracted instead of added. The other fourteen transitions are recorded only with antiparallel excitation, and the differential Doppler shift is calculated from the ion velocity.

High-resolution measurements of hfs provide, of course, a test of *ab initio* calculations, and are useful for a correct interpretation of spectra from stars, but are also necessary in order to determine accurately the isotope shifts of odd isotopes. The hyperfine structure of ten levels in the $4f^6(^7F)5d$ and $4f^5\,5d6s$? configurations have been measured in this work. The hfs of three of the levels have not ben measured before, whereas the others, which have been measured previously with the laser–ion-beam technique by Young *et al.* [15], are measured with improved accuracy.

II. EXPERIMENT

A. Experimental setup

The experimental procedure for IS and hfs measurements at the Uppsala isotope separator has been described in recent papers [10,16]. Samarium ions, some of which are occupying the metastable $4f^6(^7F)5d$ levels, are produced in an arc discharge ion source from samarium chloride in a flow of CCl_4 vapor to enhance the ion production. The ions are accelerated to an energy of 35 keV and isotopically separated by an analyzing magnet. The ions are excited from the metastable levels to levels in the $4f^5\,5d6s$? or $4f^6\,6p$? configurations by laser light from a cw ring dye laser (CR-699) pumped by an argon ion laser (INNOVA 400). Resonances are detected by observing the laser-induced fluorescence light of 350–400 nm emitted in transitions to levels in the $4f^6(^7F)6s$ ground configuration. An elliptical mirror collects the fluorescence and directs it to the entrance aperture of a photomultiplier tube. Various filters are used to suppress detection of scattered laser light. The elliptical mirror is biased with a constant potential of a couple of hundred volts defining the interaction region by Doppler tuning the laser light frequency with respect to the accelerated ions. A portion of the laser light is directed into a temperature-stabilized and sealed confocal Fabry-Pérot interferometer (FPI) providing frequency markers.

B. Measurements

The natural abundances of the samarium isotopes investigated here are ^{147}Sm 15.1%, ^{148}Sm 11.3%, ^{149}Sm 13.9%, ^{150}Sm 7.4%, ^{152}Sm 26.7%, and ^{154}Sm 22.6%. When the spectrum of one isotope has been recorded for the IS measurements, the next isotope is switched into the beam line by changing the current through the analyzing magnet. Each part of the spectrum is then isotopically pure, which can simplify the interpretation. The IS of Sm II transitions are large and the spectra from the odd and even isotopes overlap. Therefore, we have recorded the frequency shift between pairs of isotopes as shown in Fig. 1. About five recordings are made for each pair of isotopes. By adding the frequency separation between isotopes in the spectra recorded in the parallel and antiparallel geometry, respectively, the differences in the first-order Doppler shift between accelerated ions with different masses cancel. The expression for the isotope shift is [14]

$$\delta\nu_{\mathrm{IS}}=\frac{(\delta\nu_{AA'}^{\mathrm{parallel}}+\delta\nu_{AA'}^{\mathrm{antiparallel}})}{2}-Q_{AA'}\,. \tag{1}$$

$\delta\nu_{AA'}$ is the frequency separation $\nu_{A'}-\nu_A$ between reference isotope A' (154 in this work) and isotope A (147–150, 152), and $Q_{AA'}$ is a correction for the second-order differential Doppler shift. The value of $Q_{AA'}$ is typically a few MHz with an uncertainty of less than 0.1%. By subtracting the frequency differences between isotopes, the IS and $Q_{AA'}$ cancel and an expression for the ion velocity, $v_{A'}$, may be evaluated from the first-order Doppler shift difference:

$$v_{A'}=\frac{c_0(\delta\nu_{AA'}^{\mathrm{parallel}}-\delta\nu_{AA'}^{\mathrm{antiparallel}})}{\{2\nu_{A'}[1-(M_{A'}/M_A)^{1/2}]\}}\,. \tag{2}$$

The atomic masses $M_{A,A'}$ are given in [17]. The IS for the transitions recorded only with antiparallel laser and ion beams can then be calculated by use of

$$\delta\nu_{\mathrm{IS}}=\delta\nu_{AA'}^{\mathrm{antiparallel}}+\frac{\nu_{A'}v_{A'}}{c_0}\left\{1-\left[\frac{M_{A'}}{M_A}\right]^{1/2}\right\}-\frac{\nu_{A'}v_{A'}^2}{2c_0^2}\left\{1-\frac{M_{A'}}{M_A}\right\}\,. \tag{3}$$

The relative systematic uncertainty of the IS originating from the uncertainty in the ion velocity is rather small here, since the IS in Sm II is large.

The transitions we have investigated are given in Fig. 2. Energy levels and transition wavelengths are tabulated in [4,18]. The transitions at 577.89 nm (2), 592.26 nm (8), and 596.75 nm (14) could not be found in [18], but the transition at 596.75 nm (14) was observed earlier by Young *et al.* [15] (the above wavelengths have an estimated uncertainty of about ±0.01 nm). These three transitions are assigned using tabulated energy levels [4] and the assignment is supported by the observed hfs. The number of hfs components, as well as the relative intensity of the peaks, contain information about the J quantum number of the involved levels, since strong peaks belong to $\Delta F=\Delta J$ transitions. The IS's of the transitions at

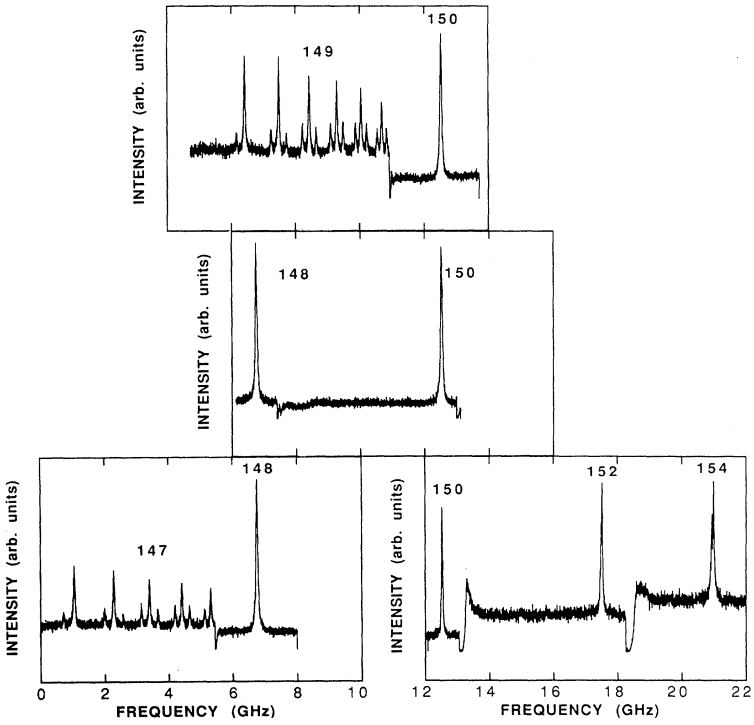

FIG. 1. IS and part of the hfs of the reference transition at 578.698 nm in Sm II recorded with antiparallel laser and ion beams.

578.698 nm (ref) and 583.102 nm (3) are recorded with both parallel and antiparallel laser and ion beams and the IS's of the other transitions are recorded only in the antiparallel geometry.

Several of the investigated transitions are weak, which is manifested by long lifetimes of the upper levels, in addition to which the transitions are not tabulated. For the weakest resonances at 577.89 nm (2) and 592.26 nm (8), with a common upper level, we observed a small peak shifted 1.5 GHz toward higher frequency from the resonances (Fig. 3) (corresponding to the -300 V of postacceleration). This small extra peak is interpreted as the fluorescence from the ions that are excited upstream from the interaction region. The fluorescence from these excited ions is observed because the upper level is long lived and has not decayed before they enter the elliptical mirror.

III. RESULTS

The positions of the frequency markers and the spectral lines are determined by curve-fitting procedures. The frequency scale is obtained in a polynomial fit of the positions of the frequency markers from the FPI. The free spectral range (FSR) of the FPI, 149.79±0.04 MHz (70% confidence interval) [10], gives a maximum systematic uncertainty of 0.026% to any measured frequency difference. The observed linewidth is about 40 MHz [full width at half maximum (FWHM)] and arises mainly from longitudinal Doppler broadening, due to the ion source energy spread, and natural lifetime broadening. The ratio of the Doppler shift correction $\Delta\nu$ to the separation

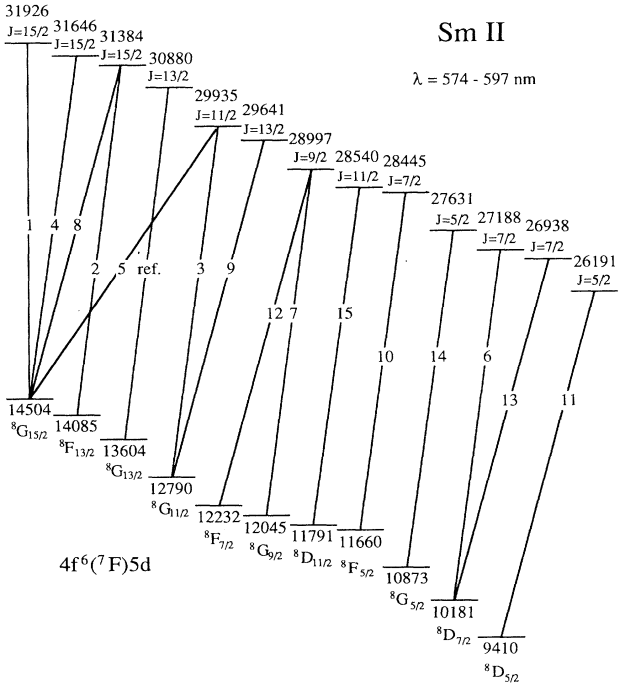

FIG. 2. Partial energy level diagram of Sm II with the transitions used indicated. The transitions are numbered after increasing transition wavelength (cf. Table II). The transition marked as ref is used as a reference in this investigation.

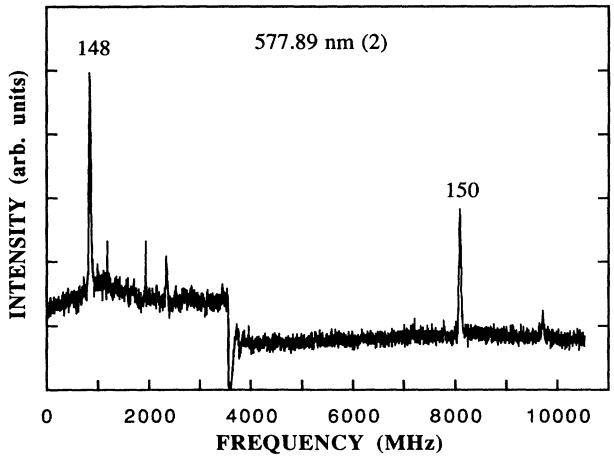

FIG. 3. Recorded frequency difference between the isotopes ^{148}Sm II and ^{150}Sm II for the transition at 577.89 nm (2). A small peak is observed 1.5 GHz toward higher frequency for both isotopes.

$\Delta\nu_0$ between hfs components is given by $\Delta\nu/\Delta\nu_0 = \pm v/c \approx \pm 0.71$ MHz/GHz (0.071%) for antiparallel (+) and parallel (−) geometry, respectively.

A and B factors are evaluted from the well known expression for the energy contributions from the magnetic-dipole and electric-quadrupole interactions [19]. The final numbers are corrected for the linear differential Doppler shift (0.071 %). This procedure is justified, since second- and higher-order corrections are negligible. For the transition at 577.89 nm (2), the known values of the hfs constants for the lower level at 14 504 cm^{-1} [15] were used when the A and B factors of the upper level at 31 383.62 cm^{-1} were derived. This is also the upper level in the transition at 592.26 nm (8) and its A and B factors were then used when the hfs constants for the lower level at 14 085 cm^{-1} in transition (8) were derived. This procedure is used because these transitions are weak and, consequently, mainly $\Delta F = \Delta J$ transitions are observed and, therefore, the number of free parameters in the fit had to be reduced. The results for the hfs are given in

TABLE I. Experimental hfs constants for the isotopes ^{147}Sm II and ^{149}Sm II ($I = \frac{7}{2}$). The levels are assigned according to [4]. The uncertainties presented within parentheses for this work are the linear sum of the statistical spread (70% confidence interval) and the estimated maximum systematic uncertainty originating from the calibration of the FSR (0.026%). The measurements are compared with earlier measurements of which the uncertainties are quoted from the references.

Isotope	Level (cm^{-1})	A (MHz)	A^{147}/A^{149}	B (MHz)	Reference
147	$4f^6(^7F)5d\ ^8D_{7/2}$	29.9(2)		−93(6)	this work
	10 180.70	29.9(5)		−88(5)	[15]
147	$4f^6(^7F)5d\ ^8G_{5/2}$	−19.16(10)		−75.5(9)	this work
	10 873.30	−19.3(5)		−78(5)	[15]
147	$4f^6(^7F)5d\ ^8G_{11/2}$	−25.65(10)	1.20(1)	−50(3)	this work
	12 789.81	−25.8(5)	1.22(3)	−46(5)	[15]
149		−21.33(10)		19(4)	this work
		−21.1(5)		21(5)	[15]
147	$4f^6(^7F)5d\ ^8G_{13/2}$	−29.27(4)	1.204(4)	−21(4)	this work
	13 604.50	−29.2(5)	1.22(3)	−26(5)	[15]
149		−24.30(5)		5(7)	this work
		−24.0(5)		3(5)	[15]
149	$4f^6(^7F)5d\ ^8F_{13/2}$	−43.23(7)		−49(2)	this work
	14 084.55				
147	$4f^5\,5d6s?\ J=\frac{7}{2}$	−78.1(2)		−5(6)	this work
	26 938.42	−78.2(5)		−2(5)	[15]
147	$4f^5\,5d6s?\ J=\frac{5}{2}$	−82.23(8)		−11.7(9)	this work
	27 631.18	−82.7(5)		−17(5)	[15]
147	$4f^5\,5d6s?\ J=\frac{11}{2}$	−144.9(2)	1.212(3)	61(6)	this work
149	29 934.80	−119.6(2)		−8(4)	this work
147	$4f^5\,5d6s?\ J=\frac{13}{2}$	−151.09(11)	1.213(1)	90(7)	this work
	30 879.74	−151.2(5)	1.216(6)	80(10)	[15]
149		−124.60(10)		−29(8)	this work
		−124.3(5)		−24(5)	[15]
149	$4f^5\,5d6s?\ J=\frac{15}{2}$	−152.16(13)		40(4)	this work
	31 383.62				

TABLE II. Experimental IS for transitions in Sm II. The uncertainties presented include both statistical spread (70% confidence interval) and the estimated maximum systematic uncertainty as discussed in the text.

Lower level and energy (cm^{-1})[a]	Upper level and energy (cm^{-1})[a]	λ_{air} (nm)[b]	Isotope A	$\delta\nu^{A,154}$ (MHz)	Δ_{stat}	Δ_{syst} (MHz)	Δ_{tot}
Transitions recorded in both the parallel and antiparallel laser–ion-beam geometry							
(ref) $4f^6(^7F)5d\ ^8G_{13/2}$	$4f^5 5d6s?\ J=\frac{13}{2}$	578.698	152	2131.4	1.0	0.6	1.6
13 604.50	30 879.74		150	6430.0	0.6	1.7	2.3
			149	8560	0.9	11	12
			148	9356.2	1.2	2.4	3.6
			147	10 821	1.4	9.5	11
(3) $4f^6(^7F)5d\ ^8G_{11/2}$	$4f^5 5d6s?\ J=\frac{11}{2}$	583.102	152	2009.4	1.2	0.5	1.7
12 789.81	29 934.80		150	6061.3	1.8	1.6	3.4
			149	8072	2.5	12	15
			148	8814.7	2.6	2.3	4.9
			147	10 245	3.5	13	17
Transitions recorded only in the antiparallel geometry where the differential Doppler shift is calculated from the ion velocity							
(1) $4f^6(^7F)5d\ ^8G_{15/2}$	$4f^5 5d6s?\ J=\frac{15}{2}$	573.801	152	2866.0			2.6
14 503.67	31 926.40		150	8718.5			7.3
			148	12 694			11
(2) $4f^6(^7F)5d\ ^8F_{13/2}$	$4f^5 5d6s?\ J=\frac{15}{2}$	577.89[c]	152	3491.1			4.8
14 084.55	31 383.62		150	10 467.6			8.8
			148	15 232			13
(4) $4f^6(^7F)5d\ ^8G_{15/2}$	$4f^5 5d6s?\ J=\frac{15}{2}$	583.174	152	3052.9			4.1
14 503.67	31 646.49		150	9163.2			7.8
			148	13 336			11
(5) $4f^6(^7F)5d\ ^8F_{9/2}$	$4f^5 5d6s?\ J=\frac{11}{2}$	584.867	152	2018.8			3.2
14 503.67	29 934.80		150	6091.8			6.4
			148	8862.6			9.4
(6) $4f^6(^7F)5d\ ^8D_{7/2}$	$4f^6(^7F)6p?\ J=\frac{7}{2}$	587.811	152	2078.2			3.6
10 180.70	27 188.30		150	6344.3			7.1
			148	9222			10
(7) $4f^6(^7F)5d\ ^8G_{9/2}$	$4f^5 5d6s?\ J=\frac{9}{2}$	589.739	152	1917.2			3.0
12 045.17	28 997.14		150	5802.8			6.3
			148	8439.4			9.1
(8) $4f^6(^7F)5d\ ^8G_{15/2}$	$4f^5 5d6s?\ J=\frac{15}{2}$	592.26[c]	152	3464.2			9.0
14 503.67	31 383.62		150	10 410			14
			148	15 161			19
(9) $4f^6(^7F)5d\ ^8G_{11/2}$	$4f^6(^7F)6p?\ J=\frac{13}{2}$	593.290	152	2053.8			4.3
12 789.81	29 640.51		150	6220.3			7.4
			148	9045			10
(10) $4f^6(^7F)5d\ ^8F_{5/2}$	$4f^5 5d6s?\ J=\frac{7}{2}$	595.582	152	1780.8			2.9
11 659.80	28 445.43		150	5413.6			6.0
			148	7871.4			8.7
(11) $4f^6(^7F)5d\ ^8D_{5/2}$	$4f^6(^7F)6p?\ J=\frac{5}{2}$	595.752	152	1685.4			5.8
9410.00	26 190.92		150	5231.1			8.4
			148	7592			11

TABLE II. (*Continued*).

(12) $4f^6(^7F)5d\ ^8F_{7/2}$	$4f^5\,5d6s?\ J=\frac{9}{2}$	596.322	152	1926.2	3.2
12 232.34	28 997.14		150	5821.5	6.8
			148	8467.2	9.6
(13) $4f^6(^7F)5d\ ^8D_{7/2}$	$4f^5\,5d6s?\ J=\frac{7}{2}$	596.571	152	1709.4	2.8
10 180.70	26 938.42		150	5308.8	6.8
			148	7703.3	9.7
(14) $4f^6(^7F)5d\ ^8G_{5/2}$	$4f^5\,5d6s?\ J=\frac{5}{2}$	596.57[c]	152	1820.5	3.8
10 873.30	27 631.18		150	5502.9	7.3
			148	8005	10
(15) $4f^6(^7F)5d\ ^8D_{11/2}$	$4f^6(^7F)6p?\ J=\frac{11}{2}$	596.882	152	2248.8	4.7
11 791.05	28 540.12		150	6784.4	7.1
			148	9873.1	9.0

[a]Reference [4].
[b]Reference [18].
[c]This transition is not tabulated in [18]. The identification is made from the energy levels in [4] (see text).

Table I together with previously published data. The uncertainty of the B factor is much larger than the uncertainty of the A factor because the contribution of B to the hfs is 10–300 times smaller.

It is expected that the ratio of A factors between the two isotopes ^{147}Sm and ^{149}Sm equals the ratio of magnetic-dipole moments μ_I between the same pair of isotopes ($I=\frac{7}{2}$ for both isotopes). Any anomaly would arise from s and $p_{1/2}$ electrons. The ratios in Table I are J independent within the experimental uncertainties. The weighted means of the ratios of A factors in this work are

$$A^{147}/A^{149}[4f^6(^7F)5d]=1.2403(33)\ ,$$

$$A^{147}/A^{149}[4f^5\,5d6s]=1.2124(9)\ .$$

Provided that CI between levels in the $4f^6(^7F)5d$ and $4f^6(^7F)6s$ configurations is negligible, the ratio $A^{147}/A^{149}[4f^6(^7F)5d]$ is expected to be equal to the ratio of magnetic-dipole moments. According to [4], the levels have high purity. The ratio $A^{147}/A^{149}[4f^6(^7F)5d]$ is therefore used in the evaluation of the anomaly for the $4f^5(^7F)5d6s$ configuration:

$$\Delta=(A^{147}/A^{149}[4f^5\,5d6s])\{A^{149}/A^{147}[4f^6(^7F)5d]\}$$

$$-1=0.0067(35)\ .$$

The result of the IS in the transitions at 578.698 nm (ref) and 583.102 nm (3), recorded with parallel as well as antiparallel laser and ion beams, is given in Table II A. The presented uncertainty is the linear sum of the statistical spread on a 70% confidence level and the estimated maximum systematic uncertainty. The systematic uncertainty originates from the uncertainty in the FSR (0.026%), and for the odd isotopes also from the estimated maximum systematic uncertainty in the center of gravity of the hyperfine multiplet.

The ion velocity of ^{154}Sm II is calculated using Eq. (2). We have used the frequency difference between even isotopes for the calibration, since the odd isotopes have larger uncertainties in the center of gravity. The statistical uncertainty of the ion velocity is 0.024%, which, together with the systematic uncertainty originating from the FSR (0.026%), gives an uncertainty of 0.050% to the calculated differential Doppler shift (the differential Doppler shifts is of the order of -7 GHz between isotopes 154 and 148), and 0.10% to the acceleration voltage. The result from the calibration of the acceleration voltage is 34.96 (4) kV, which is in good agreement with the value 34.98 kV on the acceleration voltage display (the postacceleration voltage is taken into account). The result shows that this is a suitable method to calibrate the acceleration voltage. The IS's of the transitions recorded with antiparallel laser and ion beams are calculated using Eq. (3) and the result is given in Table II B. The uncertainty presented is the linear sum of the uncertainty in the measured peak separation and the uncertainty in the calculated differential Doppler shift.

IV. INTERPRETATION OF RESULTS

A. Level shifts

Since we have measured the IS for a number of transitions with a common upper or common lower level (Fig. 2), differences in level IS can be derived for several levels. The level IS's of the lower levels are expected to be almost equal if the interaction with levels in the ground configuration $4f^6\,6s$ is negligible. It should be pointed out that the lower-level $4f^6(^7F)5d\ ^8G_{15/2}$ at 14 503.67 cm^{-1} cannot mix with levels in $4f^6(^7F)6s$, since there are no levels with $J=\frac{15}{2}$ in that configuration. From Table

TABLE III. Evaluated level IS between ^{154}Sm II and ^{148}Sm II. The second column gives the level IS from [5] of the upper levels, and the fourth column gives the transition IS from this work. The level IS's in columns 3 and 6 are calculated using our data in combination with the data in column 2 of the upper and lower levels, respectively. IS's are given in MHz.

Upper level (cm^{-1})	Level IS from [5]	Level IS (calc.)	Transition IS from this work	Lower level (cm^{-1})	Level IS (calc.)
26 190.92	7705		7592	9 410.00	113
26 938.42		7774	7703	10 180.70	71
27 188.30	9293		9222	10 180.70	71
27 631.18	8154		8005	10 873.30	149
28 445.43	8514		7871	11 659.80	643
28 540.12	7735		9873	11 791.05	−2138
28 997.14			8439	12 045.17	
			8467	12 232.34	
29 640.51	9204		9045	12 789.81	159
29 934.80		8974	8815	12 789.81	159
		8974	8863	14 503.80	111
30 879.74			9356	13 604.50	
31 383.62		15272	15222	14 084.55	40
		15272	15161	14 503.67	111
31 646.49		13447	13336	14 503.67	111
31 926.40		12805	12694	14 503.67	111

III, it is clear that the level IS for the lower levels are fairly equal, while they vary more for the upper levels. Six of the upper levels in this investigation are also investigated in [5], where the level IS between the isotopes 154 and 148 were evaluated. A number of level IS's can be calculated from our data in combination with the data in [5]. The result is given in Table III.

According to [4], all even levels investigated in this work, except $4f^6(^7F)5d\ ^8F_{5/2}$ at 11 659.80 cm^{-1}, have negligible CI. The large level IS of $^8F_{5/2}$ at 11 659.80 cm^{-1} in Table III could arise from CI, whereas this is not likely for the level $^8D_{11/2}$ at 11 791.05 cm^{-1}. A comparison with the derived level shifts in [5] and the transition IS's obtained here supports the conclusion that CI is negligible for the other lower levels. The mean level IS for these lower levels is 107 MHz.

B. King plots

The IS is assumed to be the sum of the FS, depending on the nuclear charge distribution, and the MS, caused by the difference in nuclear mass. The MS is, in turn, defined to be the sum of the NMS and the SMS. The validity of this assumption can be checked by a King diagram [20]. In a King diagram the modified residual IS ($\delta\sigma'$) for a transition α is plotted versus the modified residual IS for a reference transition for all isotopes (see, e.g., [2,3]). The modified residual IS for an isotope A is obtained by subtracting the NMS from the IS and multiplying with $[(M_{154}-M_{152})M_A/(M_{154}-M_A)M_{152}]$, where the isotope pair 154-152 is chosen to be the standard pair of isotopes in this work. The transition at 578.698 nm (ref) is taken as reference, since the IS for this transition is the most accurate. If the assumption is valid, the points follow a straight line according to

$$\delta\sigma'_\alpha=(F_\alpha/F_{\rm ref})\Delta\sigma'_{\rm ref}+\frac{(k_\alpha-k_{\rm ref}F_\alpha/F_{\rm ref})(M_{154}-M_{152})}{(M_{154}M_{152})}\ . \quad (4)$$

The slope of the line $F_\alpha/F_{\rm ref}$ is the ratio between the electronic part of the FS of the two transitions and from the intersection of the line with the y axis we obtain the parameter $(k_\alpha-k_{\rm ref}F_\alpha/F_{\rm ref})$, where k is proportional to the electronic part of the SMS. In the King plot of the transition at 583.102 nm (3), a small deviation from the line of 13 MHz, slightly larger than the experimental uncertainty of 5 MHz, is noticeable for the isotope pair ^{147,154}Sm II (Fig. 4). The deviation, if not accidental, might be an effect of second-order hyperfine interaction, which mixes levels with different total angular momentum J and shifts the center of gravity of the hfs. The effect of second-order hfs on the IS in Sm I has been observed by Brandt, Seibert, and Steudel [21] and calculated by Labarthe [22], but we have not found any estimates of this effect in Sm II. The shift is proportional to the square of the magnetic-dipole and electric-quadrupole moments, respectively, [2], and is therefore larger for ^{147}Sm than for ^{149}Sm. The King parameters for all transitions are listed in Table IV. The measurement of ^{147}Sm II is excluded in the derivation of the King parameters for the transition at 583.102 nm (3).

In order to derive absolute values of the FS and the SMS, they have to be known for one transition and then the FS and SMS for other transitions can be evaluated by means of the King parameters obtained from the data. In the case of samarium, the SMS can be determined by comparing the IS in Sm II with the IS of a pure $6s^2\rightarrow 6s6p$ transition in Sm I. A pure $6s^2\rightarrow 6s6p$ transition is expected to have a small SMS [3]. IS's of several transitions between the ground configuration $4f^6\,6s^2$ and the upper configurations $4f^6\,6s6p$ and $4f^5\,5d\,6s^2$ have

TABLE IV. King parameters and field and specific-mass shifts. The uncertainties presented within parentheses for the King parameters are the standard errors from the fits. The uncertainty for the FS and SMS originates mainly from the SMS of the $6s^2 \rightarrow 6s6p$ transition in [23].

λ_α (nm)		F_α/F_{ref}	$(K_\alpha - K_{\text{ref}}F_\alpha/F_{\text{ref}})$ $\times 2/152\cdot154$ (MHz)	$FS^{152,154}$ (MHz)	$SMS^{152,154}$ (MHz)
Sm I:	589.97	−0.4892(3)	−235.0(8)	−1266(10)	0.0(9.3)
(ref)	578.698	1	0	2587(19)	−480(19)
(1)	573.801	1.381(5)	−68(12)	3574(29)	−732(19)
(2)	577.89	1.607(3)	81(7)	4160(32)	−690(32)
(3)	583.102	0.942(1)	0(4)	2437(18)	−452(18)
(4)	583.174	1.410(2)	58(4)	3647(27)	−619(20)
(5)	584.867	0.9478(4)	−2(1)	2452(18)	−457(20)
(6)	587.811	1.0106(4)	−75(1)	2615(19)	−561(20)
(7)	589.739	0.9083(5)	−21(2)	2350(17)	−457(19)
(8)	592.26	1.607(4)	55(10)	4158(32)	−718(33)
(9)	593.290	0.9748(2)	−24(4)	2522(19)	−492(20)
(10)	595.582	0.8612(7)	−63(2)	2228(17)	−477(19)
(11)	595.752	0.86015(2)	−150.6(1)	2225(17)	−564(17)
(12)	596.322	0.9085(7)	−12(2)	2350(18)	−448(19)
(13)	596.571	0.8738(3)	−155(1)	2261(17)	−575(19)
(14)	596.57	0.8593(1)	−13.7(3)	2223(17)	−426(20)
(15)	596.882	1.0554(6)	1(2)	2731(20)	−505(21)

been accurately measured with the laser–atomic-beam technique by Brandt, Seibert, and Steudel [21]. The transition at 598.97 nm is chosen to be a pure $6s^2 \rightarrow 6s6p$ transition in Sm I, with negligible SMS. The upper level has 99.7% purity in the configuration $4f^6\,6s6p$ according to [4], which is supported by the investigation in [21]. A King diagram of this transition against the reference in Sm II gives $F(6s^2 \rightarrow 6s6p)/F_{\text{ref}} = -0.44892$ (3) and $[k(6s^2 \rightarrow 6s6p) - k_{\text{ref}}F(6s^2 \rightarrow 6s6p)/F_{\text{ref}}] = -2750$ (10) GHz amu (Fig. 5). The value $k(6s^2 \rightarrow 6s6p) = 0 \pm 9$ MHz from [21] is used in a calculation of the SMS for the reference transition. The FS of the reference transition is obtained by subtracting the SMS from the residual IS. For the other transitions, the FS is calculated from the ratio F_α/F_{ref} and the SMS is calculated by subtracting the FS from the residual IS. The results are given in Table IV. The uncertainties of the FS and SMS originate mainly from the estimated SMS of the $6s^2 \rightarrow 6s6p$ transition. It is expected that the FS is large and positive, and the SMS large and negative, for pure $4f^6\,5d \rightarrow 4f^5\,5d6s$ transitions, whereas for pure $4f^6\,5d \rightarrow 4f^6\,6p$ transitions the FS should be small and positive, and the SMS small and negative (see Appendix A). Since the level shifts of the even levels are fairly equal, the composition of the odd levels is qualitatively described in the plot of the FS against the SMS in Fig. 6 and hence no clear distinction between transition IS and level IS of the upper levels is used in the following.

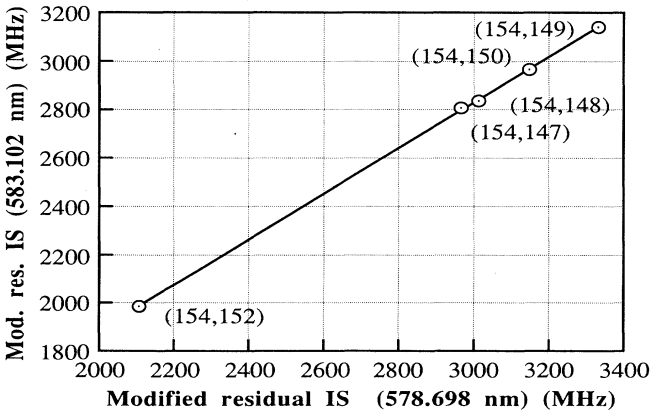

FIG. 4. King diagram of the modified residual isotope shifts of the transition at 583.102 nm (3) against the reference transition at 578.698 nm in Sm II. A small deviation from the straight line is observed for the isotope ^{147}Sm II.

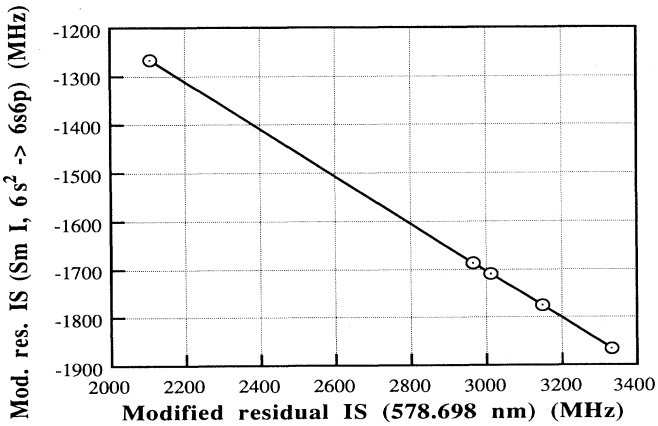

FIG. 5. King diagram of the modified residual isotope shifts of the $4f^6 6s^2 \rightarrow 4f^6\,6s6p$ transition at 598.97 nm in Sm I against the reference transition at 578.698 nm in Sm II.

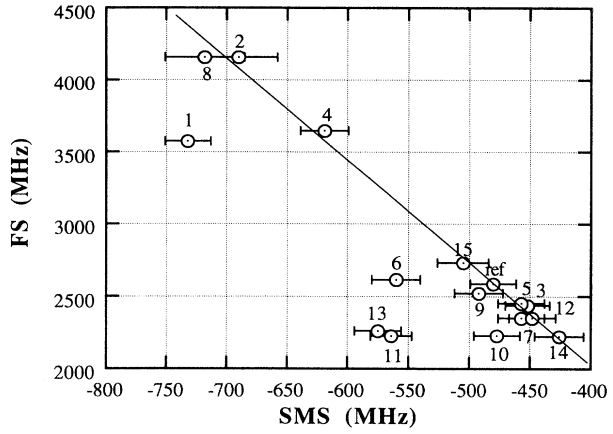

FIG. 6. The field shift as a function of the specific-mass shift for the Sm II lines investigated in this work.

C. Sharing rule

In a first approximation, the IS for all levels within a pure configuration are equal. Then the IS of a level in a mixed configuration equals the sum of the IS's of pure configurations ΔT_i multiplied by the mixing coefficients c_i according to the sharing rule [2]:

$$\Delta\nu_{\mathrm{IS}}=\Sigma_i c_i\Delta T_i$$
$$=\Sigma_i c_i(\Delta\nu^i_{\mathrm{FS}}+\Delta\nu^i_{\mathrm{SMS}}+\Delta\nu^i_{\mathrm{NMS}})\ ,\quad \Sigma_i c_i=1\ . \tag{5}$$

For a mixing of two configurations, $\Delta\nu_{\mathrm{IS}}=c_1\Delta T_1+(1-c_1)\Delta T_2$ and thus the IS, the FS, and the SMS all have the same linear dependence on the mixing coefficient c_1. A plot of FS versus SMS should then give a straight line if the levels are composed of two configurations. This is valid for the data in Ref. [23]. From this straight line it is possible to derive the mixing coefficients provided that the FS or SMS is known of the pure configurations. An investigation of this type is presented in [24]. It is clear from the plot in Fig. 6 that the sharing rule for two configurations is not valid for all transitions in this investigation and we will therefore extend the treatment to include the $4f^5\,5d^2$ configuration. CI of the odd levels with the $4f^5\,5d^2$ levels was already suggested in [5].

The FS in a $4f^5\,5d6s\rightarrow 4f^5\,5d^2$ transition is large and negative due to the $6s$-electron transition. The SMS for the $4f^6\,6s\rightarrow 4f^6\,5d$ transition is determined by Brandt, Seibert, and Steudel [6] for a change of two neutrons to be -30 ± 60 MHz. The SMS for the $4f^5\,5d6s\rightarrow 4f^5\,5d^2$ transition is approximately the same (see Appendix A and [2]) and, therefore, essentially zero. Hence, any small admixture of $4f^5\,5d^2$ in $4f^5\,5d6s$ is expected to reduce the FS considerably and the SMS hardly at all.

The $4f^6\,6p\rightarrow 4f^5\,5d^2$ transition gives a small positive FS due to less screening of the $5s$ electrons in the $4f^5\,5d^2$ configuration, whereas the SMS is expected to be large and negative due to the $4f$ electron transition (see Appendix A). An admixture of $4f^5\,5d^2$ in $4f^6 6p$ should then increase the FS slightly and reduce the SMS considerably. Deviations from a straight line for the plot of the SMS versus the FS are obvious in Fig. 6.

The transition IS, in our case with a pure lower configuration, may be expressed as

$$\Delta\nu_{\mathrm{IS}}=x\Delta T(4f^6\,6p)+(1-x)[y\Delta T(4f^5\,5d6s)$$
$$+(1-y)\Delta T(4f^5\,5d^2)]-\Delta T(4f^6\,5d)\ , \tag{6}$$

where $x,y=[0-1]$. The values $\Delta T(4f^5\,5d6s)=15\,289$ MHz, $\Delta T(4f^5\,5d^2)=4647$ MHz, and $\Delta T(4f^6\,6p)=1799$ MHz are given in [5]. $\Delta T(4f^6\,5d)=107$ MHz is the mean of the level shifts derived in Table III. The IS is plotted as a function of the composition of $4f^6\,6p$ (x) in Fig. 7 for different values of y. The diagram is a triangle with the IS for the pure configurations in each corner, IS for mixing of two configurations along the sides, and IS for mixing of three configurations in the plane spanned by the triangle. $y=1$ (no contribution from $4f^5\,5d^2$) for the points on the line in Fig. 6 and we can therefore derive the composition $[x4f^6\,6p+(1-x)4f^5\,5d6s]$ of the upper levels using the sharing rule (excluding transitions 1, 6, 9, 10, 11, and 13), i.e., Eq. (6) reduced to $\delta\nu_{\mathrm{IS}}=1799x+15\,289(1-x)-107$ if we insert the numerical values of the ΔT_i:s. For instance, the level at 31 384 cm^{-1} turns out to be pure $4f^5\,5d6s$,[1] i.e., $x=0$, $y=1$. Transitions below the line in Fig. 6 have an upper level that contains a mixing of three configurations. However, from the discussion above, it is clear that any change in the SMS must depend only on an admixture of $4f^6\,6p$

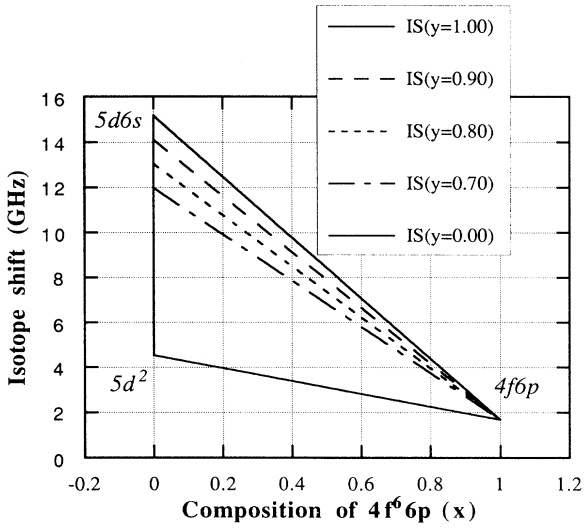

FIG. 7. The transition IS as a function of the composition of $4f^6\,6p$ in the upper level for different values of y: $\mathrm{IS}=x\Delta T(4f^6\,6p)+(1-x)[y\Delta T(4f^5\,5d6s)+(1-y)\Delta T(4f^5\,5d^2)]-\Delta T(4f^6\,5d)$.

[1]The $4f\rightarrow 6s$ one-electron transition is not allowed. Therefore, the level cannot be 100% pure. However, the transition is very weak and, within the uncertainty of the compositions derived in this work, we can say that it is close to 100% pure.

TABLE V. Assignments of the upper levels from literature and tentative compositions, $(1-x)y|4f^5 5d6s\rangle+x|4f^6 6p\rangle+(1-x)(1-y)|4f^5 5d^2\rangle$, from this work. The estimated uncertainty is 8%.

Energy (cm^{-1})	J	Assignment in [4]	Composition from [5]	Tentative composition from this work (%) $4f^5 5d6s$ $100(1-x)y$	$4f^6 6p$ $100x$	$4f^5 5d^2$ $100(1-x)(1-y)$
26 190.92	5/2	$4f^6 6p$	$4f^6 6p$	36	27	27
26 938.42	7/2	$4f^5 5d6s$		36	24	40
27 188.30	7/2	$4f^6 6p$	$4f^5 5d6s$ + other	51	27	22
27 631.18	5/2	$4f^5 5d6s$	$4f^5(5d6s+5d^2)+4f^6 6p$	47	53	
28 445.43	7/2	$4f^5 5d6s$	$4f^5(5d6s+5d^2)+4f^6 6p$	43	44	13
28 540.12	11/2	$4f^6 6p$	$4f^6 6p$	61	39	
28 997.14	9/2	$4f^5 5d6s$		50	50	
29 640.51	13/2	$4f^6 6p$	$4f^5 5d6s$	53	41	6
29 934.80	11/2	$4f^5 5d6s$		53	47	
30 879.74	13/2	$4f^5 5d6s$		57	43	
31 383.62	15/2	$4f^5 5d6s$		100		
31 646.49	15/2	$4f^5 5d6s$		87	13	
31 926.40	15/2	$4f^5 5d6s$		75		25

(and not on $4f^5 5d^2$) and, hence, the level at 31 926 cm^{-1} (transition 1) must have $x=0$ and $y\neq 1$. y can then easily be obtained from $\Delta\nu_{IS}=y\Delta T(4f^5 5d6s)+(1-y)\Delta T(4f^5 5d^2)-\Delta T(4f^6 5d)$. Similarly, for all other transitions below the line $y=1$, x can first be obtained from the SMS alone and y then from Eq. (6). The results are listed in Table V and a more detailed discussion on this procedure is found in Appendix B. The estimated uncertainty of the composition is 8% and originates from the uncertainty in FS (1%), SMS (5%), and from ΔT (2%) [5].

V. DISCUSSION

In this work, we have presented accurate measurements of hfs and IS in Sm II. For the hfs measurements, we have obtained improved accuracy and the results are in good agreement with earlier measurements. The transition IS's measured here have, to our knowledge, not been measured previously. Our approach to using an isotopically pure ion beam and switching consecutive isotopes into the beam line within a laser scan for the IS measurements is advantageous when there is an overlap between the spectra from different isotopes, since it simplifies the determination of the peak positions. An approach to the absolute calibration of the acceleration voltage is presented. The achieved accuracy of 0.1% compares well with accuracies obtained with other methods. Tentative compositions of the upper levels are evaluated from derived FS and SMS using the sharing rule. The result confirms the assignment in [5] in most cases.

Finally, the work points out the need for further development of *ab initio* calculations of the wave functions of heavy many-electron atoms. The knowledge of the electronic structure of Sm II is far from complete, but systematic experimental and theoretical investigations could be expected to lead to new insights into the many-electron system.

ACKNOWLEDGMENTS

This work was supported by the Swedish Natural Science Research Council (NFR) and the Knut and Alice Wallenberg foundation.

APPENDIX A

This appendix describes qualitatively isotope effects in pure configurations. The isotope shift (IS) is assumed to be separable into the field shift (FS) and the mass shift (MS), the latter divided into the specific mass shift (SMS) and the normal mass shift (NMS)

$$\delta\nu=\delta\nu_{FS}+\delta\nu_{MS}=F\lambda^{AA'}+\frac{M_A-M_{A'}}{M_A M_{A'}}(k_{NMS}+k_{SMS})\ . \tag{A1}$$

In a first approximation, the term dependence of the SMS is neglected, i.e., we assume that the differences between the isotope shifts of the centers of gravity of the configurations are much larger than the parameters describing the changes inside pure configurations [2]. The formal expansion for the configuration average of the SMS is given by

$$k_{SMS}=\sum_n\sum_{n'}\frac{2lNN'}{(4l+2)(4[l-1]+2)}J^2(nl,n'[l-1])\ , \tag{A2}$$

where N is the number of nl electrons, N' the number of $n'[l-1]$ electrons, and $J(nl,n'[l-1])$ the Vinti integral [25]. The sum is taken over all pairs of complete and incomplete subshells. It is straightforward to calculate the angular part of Vinti's k factor and, hence, express the SMS for the configurations of interest here as a function of the square of the Vinti integrals.

The electronic part of the FS is proportional to the

electron density at the nucleus $|\Psi(0)|^2$. In first-order perturbation theory, F is expressed as

$$F \propto \sum_n q_{ns}|\Psi_{ns}(0)|^2 , \tag{A3}$$

where q_{ns} is the number of ns electrons present in that state. The relativistic contribution from $np_{1/2}$ electrons is omitted here. Screening is accounted for by screening factors in the following way:

$$|\Psi(0)|^2_{4f^6 5d} = \chi'^6_{4f}\chi'_{5s}\chi'_{5d}2|\Psi(0)|^2_{5s} , \tag{A4a}$$

$$|\Psi(0)|^2_{4f^6 6p} = \chi'^6_{4f}\chi'_{5s}\chi_{6p}2|\Psi(0)|^2_{5s} , \tag{A4b}$$

$$|\Psi(0)|^2_{4f^5 5d6s} = \chi^5_{4f}\chi_{5d}|\Psi(0)|^2_{6s} + \chi'^5_{4f}\chi'_{6s}\chi'_{5s}\chi'_{5d}2|\Psi(0)|^2_{5s} , \tag{A4c}$$

$$|\Psi(0)|^2_{4f^5 5d^2} = \chi'^5_{4f}\chi'_{5s}\chi'^2_{5d}2|\Psi(0)|^2_{5s} , \tag{A4d}$$

where the shielding of inner s electrons by $4f$, $5s$, $6s$, $5d$, and $6p$ electrons has been neglected. $\chi=1$ is no screening and $\chi=0$ is full screening.

A qualitative estimate of the SMS and the FS for the different types of transitions involved is obtained by taking the difference between the SMS and the FS for the configurations involved.

1. $4f^6 5d \rightarrow 4f^5 5d6s$

$$M_{\mathrm{SMS}} \propto -(3/7)J^2(4f,nd) - (3/70)J^2(4f,5d) + J^2(np,6s) , \tag{A5a}$$

$$F_i \propto \chi^5_{4f}\chi_{5d}|\Psi(0)|^2_{6s} + (\chi'_{6s}-\chi'_{4f})\chi'^5_{4f}\chi_{5s}\chi'_{5d}2|\Psi(0)|^2_{5s} . \tag{A5b}$$

The SMS is expected to be large and negative because we have a reduction in the number of $4f$ electrons (which couple strongly with the nd electrons [26]). The coupling of the $6s$ electron to other electrons is weak. The FS is expected to be large and positive due to the $6s$ electron but also because of the loss of a screening $4f$ electron.

2. $4f^6 5d \rightarrow 4f^6 6p$

$$M_{\mathrm{SMS}} \propto -(9/35)J^2(4f,5d) - (2/5)J^2(5d,np) + (2/3)J^2(nd,6p) + (1/3)J^2(6p,ns) , \tag{A6a}$$

$$F_i \propto (\chi'_{6p}-\chi'_{5d})\chi^6_{4f}\chi_{5s}2|\Psi(0)|^2_{5s} . \tag{A6b}$$

The SMS is expected to be small and negative because the $5d$ electron couples more strongly with np electrons than the $6p$ electron couples to ns electrons. The contributions from the other integrals are expected to be small. The FS is expected to be small and positive if the $5d$ electron shields more than the $6p$ electron.

3. $4f^6 5d \rightarrow 4f^5 5d^2$

$$M_{\mathrm{SMS}} \propto -(3/7)J^2(4f,nd) + (6/35)J^2(4f,5d) + (2/5)J^2(5d,np) , \tag{A7a}$$

$$F_i \propto (\chi'_{5d}-\chi'_{4f})\chi'^5_{4f}\chi_{5s}\chi'_{5d}2|\Psi(0)|^2_{5s} . \tag{A7b}$$

The SMS is expected to be large and negative. The $4f$ electron couples strongly with the nd electrons but the SMS is slightly compensated in this transition by the presence of the $5d$ electron, which couples fairly strongly with inner p electrons. The FS is expected to be positive if the $4f$ electron shields more than the $5d$ electron [2].

APPENDIX B

The transition isotope shift (IS) can be expressed as

$$\Delta\nu_{\mathrm{IS}} = x\Delta T(4f^6 6p) + (1-x)[y\Delta T(4f^5 5d6s) + (1-y)\Delta T(4f^5 5d^2)] - \Delta T(4f^6 5d) , \tag{B1}$$

where $x,y=[0-1]$ and $\Delta T(4f^6 6p)=1799$ MHz, $\Delta T(4f^5 5d6s)=15\,289$ MHz, $\Delta T(4f^5 5d^2)=4647$ MHz [5], and $\Delta T(4f^6 5d)=107$ MHz.

For the points on the line in Fig. 6, we assume that $y=1$, which is consistent with $\Delta T(4f^5 5d6s)=15\,289$ MHz and the fact that no data points exist above that line, and we can derive the composition of the upper levels using the sharing rule (excluding transitions 1, 6, 9, 10, 11, and 13) from

$$\Delta\nu_{\mathrm{IS}} = x\Delta T(4f^6 6p) + (1-x)\Delta T(4f^5 5d6s) - \Delta T(4f^6 5d) , \text{ i.e. ,} \tag{B2}$$

$$x = \frac{\Delta T(4f^5 5d6s) - \Delta T(4f^6 5d) - \Delta\nu_{\mathrm{IS}}}{\Delta T(4f^5 5d6s) - \Delta T(4f^6 6p)} = \frac{15\,182 - \Delta\nu_{\mathrm{IS}}}{13\,490} . \tag{B3}$$

The result is shown in Table VI below.

For these transitions, it is also possible to calculate a one-to-one correspondence between the SMS, the FS, and x. The results, using linear regression, are

TABLE VI. The composition $x4f^6 6p + (1-x)4f^5 5d6s$ calculated from Eq. (3). The IS's are given in MHz and the upper level energy in cm^{-1}.

Trans	Upper level	IS	FS	SMS	x
2	31 383	15 222	4160	−690	0
8	31 383	15 222	4158	−718	0
4	31 646	13 336	3647	−619	0.13
15	28 540	9 873	2731	−505	0.39
ref	30 879	9 356	2587	−480	0.43
13	29 934	8 815	2437	−452	0.47
5	28 997	8 439	2350	−457	0.50
7	28 997	8 439	2350	−448	0.50
14	27 631	8 005	2223	−426	0.53

$$\Delta\nu_{\mathrm{FS}} = -3619(22)x + 4147(9) , \tag{B4a}$$

$$\Delta\nu_{\mathrm{SMS}} = 508(17)x - 699(7) , \tag{B4b}$$

$$\Delta\nu_{\mathrm{SMS}} = -0.1405(41)\Delta\nu_{\mathrm{FS}} - 116(12) . \tag{B4c}$$

For the points in the plane below the line in Fig. 6 it is clear that Eq. (B1) cannot be used as it stands (or with inserted numbers),

$$\Delta\nu_{\mathrm{IS}} = 1799x + (1-x)[15\,289y + 4647(1-y)] - 107 , \tag{B5}$$

because without any other knowledge, for any given transition isotope shift IS, we obtain a set of solutions defined by the equation

$$y = \frac{\left[\dfrac{\Delta\nu_{\mathrm{IS}} - 1799x + 107}{(1-x)} - 4647\right]}{10\,642} , \tag{B6}$$

where, of course, there is a constraint that $0 \le x \le 1$ and $0 \le y \le 1$. However, according to the sharing rule, Eq. (B1) holds also if we look at the SMS, or the FS, separately, i.e.,

$$\Delta\nu_{\mathrm{SMS}} = x\Delta\nu_{\mathrm{SMS}}^{4f^6 6p} + (1-x)[y\Delta\nu_{\mathrm{SMS}}^{5d6s} + (1-y)\Delta\nu_{\mathrm{SMS}}^{5d^2}] - \Delta\nu_{\mathrm{SMS}}^{4f^5 5d} \tag{B7a}$$

$$\Delta\nu_{\mathrm{FS}} = x\Delta\nu_{\mathrm{FS}}^{4f^6 6p} + (1-x)[y\Delta\nu_{\mathrm{FS}}^{5d6s} + (1-y)\Delta\nu_{\mathrm{FS}}^{5d^2}] - \Delta\nu_{\mathrm{FS}}^{4f^5 5d} . \tag{B7b}$$

Recollecting the discussion in Appendix A, the SMS for a $4f^6 5d - 4f^6 6p$ transition is small and negative, for a $4f^6 5d - 4f^5 5d^2$ large and negative, and for a $4f^6 5d - 4f^5 5d6s$ large and negative. However, the SMS for the $4f^6 6s - 4f^6 5d$ "transition" has been determined by Brandt, Meissner, and Steudel [6] to -30 ± 60 MHz and the SMS for a $4f^5 5d6s - 4f^5 5d^2$ transition is approximately the same, i.e., essentially zero. Hence, the SMS observed does not depend at all on the mixture of $4f^5 5d6s$ and $4f^5 5d^2$ but only on the amount of $4f^6 6p$, or, rewriting the expression for the SMS above,

$$\begin{aligned}\Delta\nu_{\mathrm{SMS}} &= x\Delta\nu_{\mathrm{SMS}}^{4f6p} + (1-x)[\Delta\nu_{\mathrm{SMS}}^{5d6s} + (1-y)\Delta\nu_{\mathrm{SMS}}^{5d^2} - \Delta\nu_{\mathrm{SMS}}^{4f5d}] \\ &\approx x\Delta\nu_{\mathrm{SMS}}^{4f6p} + (1-x)[\Delta\nu_{\mathrm{SMS}}^{5d6s} + (1-y)\Delta\nu_{\mathrm{SMS}}^{5d6s} - \Delta\nu_{\mathrm{SMS}}^{4f5d}] \\ &= x\Delta\nu_{\mathrm{SMS}}^{4f6p} + (1-x)\Delta\nu_{\mathrm{SMS}}^{4f5d} .\end{aligned} \tag{B8}$$

Hence, the mixing factor x is determined solely by the SMS and rewriting (B8) as

$$\Delta\nu_{\mathrm{SMS}} = (\Delta\nu_{\mathrm{SMS}}^{4f6p} - \Delta\nu_{\mathrm{SMS}}^{5d6s})x + (\Delta\nu_{\mathrm{SMS}}^{5d6s} - \Delta\nu_{\mathrm{SMS}}^{4f5d}) \tag{B9}$$

we see that this is the same as Eq.(5). Solving for x instead we obtain

$$x = 1.9507\ (64)\ 10^{-3}\Delta\nu_{\mathrm{SMS}} + 1.366\ (34) . \tag{B10}$$

The result is shown in Table VII. Also, y can be expressed as a function of the SMS only:

$$y = \frac{\dfrac{(\Delta\nu_{\mathrm{IS}} - 3.509\Delta\nu_{\mathrm{SMS}} - 2350)}{(-1.950710^{-3}\Delta\nu_{\mathrm{SMS}} - 0.366)} - 4647}{10642} . \tag{B11}$$

The results above are summarized in Table V.

TABLE VII. x (the fraction of $4f^6 6p$) calculated from Eq. (13) and y calculated from Eq. (8). The fractions of $4f^5 5d6s$ and $4f^5 5d^2$ are then $(1-x)y$ and $(1-x)(1-y)$, respectively. The IS's are given in MHz and the upper level energy in cm^{-1}.

Trans	Upper level	IS	SMS	x	$(1-x)y$
6	27 188	9 222	−561	0.27	0.51
9	29 640	9 045	−492	0.41	0.53
10	28 445	7 871	−477	0.44	0.43
11	26 190	7 592	−564	0.27	0.36
13	26 938	7 703	−575	0.24	0.36
1	31 926	12 694	−732	−0.06[2]	0.75

[1] E. W. Otten, *Nuclei Far from Stability,* Treatise on Heavy-Ion Science Vol. 8, edited by D. A. Bromley (Plenum, New York, 1989), p. 517.

[2] J. Bauche and R.-J. Champeau, Adv. At. Mol. Phys. **12**, 39 (1976).

[3] P. Aufmuth, K. Heilig, and A. Steudel, At. Data Nucl. Data Tables **37**, 455 (1987).

[4] *Atomic Energy Levels, The Rare Earth Elements,* Natl. Bur. Stand. (U.S.), edited by W. C. Martin, R. Zalubas, and L. Hagan (U.S. GPO, Washington, D.C., 1978), Vol. 60, p. 174.

[5] M. Pushpa, M. Rao, S. A. Ahmad, A. Venugopalan, and G. D. Saksena, Z. Phys. D **15**, 211 (1990).

[6] H. W. Brandt, E. Meissner, and A. Steudel, Z. Phys. A **291**, 97 (1979).

[7] S. A. Ahmad, M. Pushpa, M. Rao, and G. D. Saksena, Z. Phys. D **6**, 227 (1987).

[8] S. L. Kaufman, Opt. Commun. **17**, 309 (1976).

[9] W. H. Wing, G. A. Ruff, W. E. Lamb, Jr., and J. J. Spezeski, Phys. Rev. Lett. **36**, 1488 (1976).

[10] P. Villemoes, A. Arnesen, F. Heijkenskjöld, and A. Wännström, J. Phys. B **26**, 4289 (1993).

[11] O. Poulsen, Nucl. Instrum. Methods **202**, 503 (1982).

[12] L. Ward, O. Vogel, A. Arnesen, R. Hallin, and A. Wännström, Phys. Scr. **31**, 161 (1985).

[13] S. Wei, L. Fuquan, W. Songmao, S. Peixiong, Y. Jianjun, S. Linggen, T. Jiayong, and Y. Fuija, Phys. Rev. A **43**, 1451 (1991).

[14] G. Borghs, P. De Bisschop, J. M. Van den Cruyce, M. Van Hove, and R. E. Silverans, Opt. Commun. **38**, 101 (1981).

[15] L. Young, W. J. Childs, H. G. Berry, C. Kurtz, and T. Dinneen, Phys. Rev. A **36**, 2148 (1987).

[16] P. Villemoes, R. van Leeuwen, A. Arnesen, F. Heijkenskjöld, A. Kastberg, M. O. Larsson, and S. A. Kotochigova, Phys. Rev. A **45**, 6241 (1992).
[17] A. H. Wapstra and K. Bos, At. Data Nucl. Data Tables **19**, 177 (1977).
[18] *Wavelengths and Transition Probabilities for Atoms and Atomic Ions,* Natl. Bur. Stand. (U.S.), edited by J. Reader, C. H. Corliss, W. L. Wiese, and G. A. Martin (U.S. GPO, Washington, D.C., 1980), Vol. 68, p. 127.
[19] H. Kopfermann, *Nuclear Moments* (Academic, New York, 1958).
[20] W. H. King, J. Opt. Soc. Am. **53**, 638 (1963).
[21] H. Brandt, B. Seibert, and A. Steudel, Z. Phys. A **296**, 281 (1980).
[22] J. J. Labarthe, J. Phys. B **11**, L1 (1978).
[23] W. J. Childs, Phys. Rev. A **6**, 2011 (1972).
[24] P. Hannaford, R. J. McLean, and W. J. Rowland (unpublished).
[25] J. P. Vinti, Phys. Rev. **56**, 1120 (1939).
[26] W. H. King, A. Steudel, and M. Wilson, Z. Phys. **265**, 207 (1973).